Front. Earth Sci. 2016, 10(2): 292–302
DOI 10.1007/s11707-016-0552-9

RESEARCH ARTICLE

Reconstructing rice phenology curves with frequency-based analysis and multi-temporal NDVI in double-cropping area in Jiangsu, China

Hongshuo WANG[1,2], Hui LIN (✉)[2,3], Darla K. MUNROE[4], Xiaodong ZHANG[1], Pengfei LIU[5]

1 College of Information and Electrical Engineering, China Agricultural University, Beijing 100083, China
2 Institute of Space and Earth Information Science, The Chinese University of Hong Kong, Hong Kong, China
3 Department of Geography and Resource Management, The Chinese University of Hong Kong, Hong Kong, China
4 Department of Geography, The Ohio State University, Columbus, OH 43210, USA
5 School of Mathematics and Statistics, Jiangsu Normal University, Xuzhou 221116, China

Abstract Crop phenology retrieval in the double-cropping area of China is of great significance in crop yield estimation and water management under the influences of global change. In this study, rice phenology in Jiangsu Province, China was extracted from multi-temporal MODIS NDVI using frequency-based analysis. Pure MODIS pixels of rice were selected with the help of TM images. Discrete Fourier Transformation (DFT), Discrete Wavelet Transformation (DWT), and Empirical Mode Decomposition (EMD) were performed to decompose time series into components of different frequencies. Rice phenology in the double-cropping area is mainly located on the last 2 IMFs of EMD and the first 2−3 frequencies of DFT and DWT. Compared with DFT and DWT, EMD is limited to fewer frequencies. Multi-temporal MODIS NDVI data combined with frequency-based analysis can retrieve rice phenology dates with on average 79% valid estimates. The sorting result for effective estimations from different methods is DWT (85%) > EMD (80%) > DFT (74%). Planting date (88%) is easier to estimate than harvesting date (70%). Rice planting date is easily affected by the former cropping mode within the same year in a double-cropping region. This study sheds light on understanding crop phenology dynamics in the frequency domain of multi-temporal MODIS data.

Keywords discrete Fourier transformation, discrete wavelet transformation, empirical mode decomposition, rice phenology, double-cropping

Received January 20, 2015; accepted August 4, 2015

E-mail: huilin@cuhk.edu.hk

1 Introduction

Recent modeling results suggest that climate change may potentially threaten food security in the near future (Schmidhuber and Tubiello, 2007; Lobell et al., 2008). In order to forecast regional changes in food supply in the face of climate change, accurate and timely methods of crop yield monitoring are needed. One key component of crop yield estimation is crop phenology monitoring in particular, as crop phenology dynamics reflect crop responses to climate change (Raddatz and Cummine, 2003). Crop phenology monitoring at a regional scale can provide useful information for agricultural management to enhance crop yield via irrigation regulation or adjustments in crop cultivation systems. Because China feeds about 22% of the world's population with only 7% of its arable land, ensuring food security in a context of climate change in China is a pressing issue (Wang et al., 2015). The Chinese government has attached great importance to crop yield monitoring in various ways using remote sensing technologies (Genovese et al., 2001; Mo et al., 2005). This paper presents an analysis using remote sensing data to retrieve crop phenology information with frequency-based methods to facilitate crop yield monitoring in the double-cropping area of China.

Rice is a major staple crop, found on most arable land within China. Given current population growth trends, an estimated 20% more rice production is needed by 2030 in order to meet domestic needs (Peng et al., 2009). A recent study demonstrated that temperature increases in China have shifted rice phenology and affected rice yields between 1981−2000 (Tao et al., 2006). Most of the

croplands in subtropical regions are characterized by a double-cropping mode; therefore, agricultural management is more complicated than that of a single-cropping pattern. In order to estimate yields and water requirements in a context of climate change, retrieving accurate rice phenology information within a double-cropping system is a major research priority (Tan and Shibasaki, 2003).

Due to their large spatial coverage and repeated temporal sampling, remote sensing data have been widely used to detect vegetation dynamics (Chan and Xu., 2013; Wang et al., 2014), especially vegetation phenology in recent decades under the influences of climatic change (Justice et al., 1985; Cleland et al., 2007; Carrao et al., 2010). Among all satellite data used for phenology monitoring, Normalized Differential Vegetation Index (NDVI) and Enhanced Vegetation Index (EVI) are the two practical indicators that can characterize variations in greenness in growth cycles of vegetation. Due to easier accessibility from different satellite sensors, e.g., MODIS and AVHRR, NDVI has been widely used to extract phenological information such as early onset of green stage (Slayback et al., 2003; Delbart et al., 2006) and leaf shedding (Ito et al., 2008). Particularly, crop phenology (You et al., 2013) retrieved from multi-temporal NDVI can help us anticipate food security issues in a context of climate change. However, NDVI time series are easily contaminated by noise resulting from sensor view angle effects, and residual cloud and aerosol contamination (Huete et al., 2002). Such noise can result in the misidentification of phenology features such as start of greenness, peak of growing season, length of growing season, and phenology variations (Kobayashi and Dye, 2005).

As many important phenology features are easily identified in the frequency domain of NDVI time series, we often study signals in the frequency domain. Compared with non-frequency analysis, frequency-based analysis can determine both the dominant modes of phenology and the variability of those modes over time (Torrence and Compo, 1998; Qian and Chen, 1999; Huang and Shen, 2005). The main features of crop phenology can be reconstructed from different frequencies. The most well-known frequency-based methods use Fourier algorithms (Andres et al., 1994). However, Fourier analysis is appropriate for periodic or stationary data analysis, but it is not strong in depicting localized features such as crop growth within a short period (Percival and Walden, 2006). Later, wavelet analysis was adopted (Sakamoto et al., 2005; Lu et al., 2007; Wang et al., 2012b), as it can be used for non-stationary data analysis, and may better capture these localized features (Ivanov et al., 1996; Santoso et al., 1996), but it is not adaptive (Huang et al., 1998), as wavelet analysis is restricted to the mother functions and decomposing scales. Recently, Empirical Mode Decomposition (EMD) can decompose time series data into a finite and often small number of Intrinsic Mode Functions (IMFs). The starting point of EMD is to consider signals at the level of their local oscillations (Molla et al., 2006). EMD has been widely used to analyze time series in earth system science applications, e.g., seismic data analysis (Vasudevan and Cook, 2000), solar cycle in the stratosphere (Coughlin and Tung, 2004), and rainfall time series analysis (Molla et al., 2006). Previous studies have used different frequency-based methods to reconstruct crop phenology curves in various world regions. However, a comprehensive comparison among different frequency-based methods (e.g., DFT, DWT, and EMD) on crop phenology monitoring is needed as the three methods are fundamental for time series analysis in remote sensing.

Sakamoto et al. (2005) adopted the DWT method to study rice phenology in Japan. Sakamoto et al. (2006) and Chen et al. (2011, 2012) used DWT and EMD methods respectively to study rice phenology in the Mekong Delta. Relatively few studies to date have obtained rice phenology features for the subtropical regions in China (Wang et al., 2012a), where cropping systems exhibit unique patterns due to limited arable land and sporadic distributions. Land tenure in China is subject to the 'Household Responsibility System', which results in many small parcelized croplands with quite different cropping systems compared to those of industrialized agriculture (Shen et al., 2011). Thus, it is a big challenge to monitor rice phenology in double-cropping areas in China with robust methods.

In this study, the three phenology-monitoring methods (DFT, DWT, and EMD) were adopted to monitor rice phenology in the double-cropping area of Jiangsu Province, China. We selected pure MODIS pixels of rice, and then retrieved the key rice phenology curves by decomposing original NDVI time series into various frequencies using DFT, DWT, and EMD. We propose different methodological schemes to reconstruct the intra-annual rice phenology curves from information in the frequency domain. We discuss the advantages and shortcomings of different methods in reconstructing rice phenology curves in the double-cropping area.

2 Study area

The study area is located in Jiangsu Province, China (Fig. 1), where it is characterized primarily by plains and belongs to a subtropical monsoon climate meteorologically. More than 90% of the study area is covered by croplands (Fig. 1), predominantly rice (Xiao et al., 2005), and the paddy fields are spatially continuous. Thus it is possible to select pure rice-covered MODIS pixels (250 m $\times$ 250 m) in this region. According to the ground agricultural observations from the China Meteorological Data Sharing Service System, the intra-annual double-cropping mode is mainly wheat-rice or rapeseed-rice.

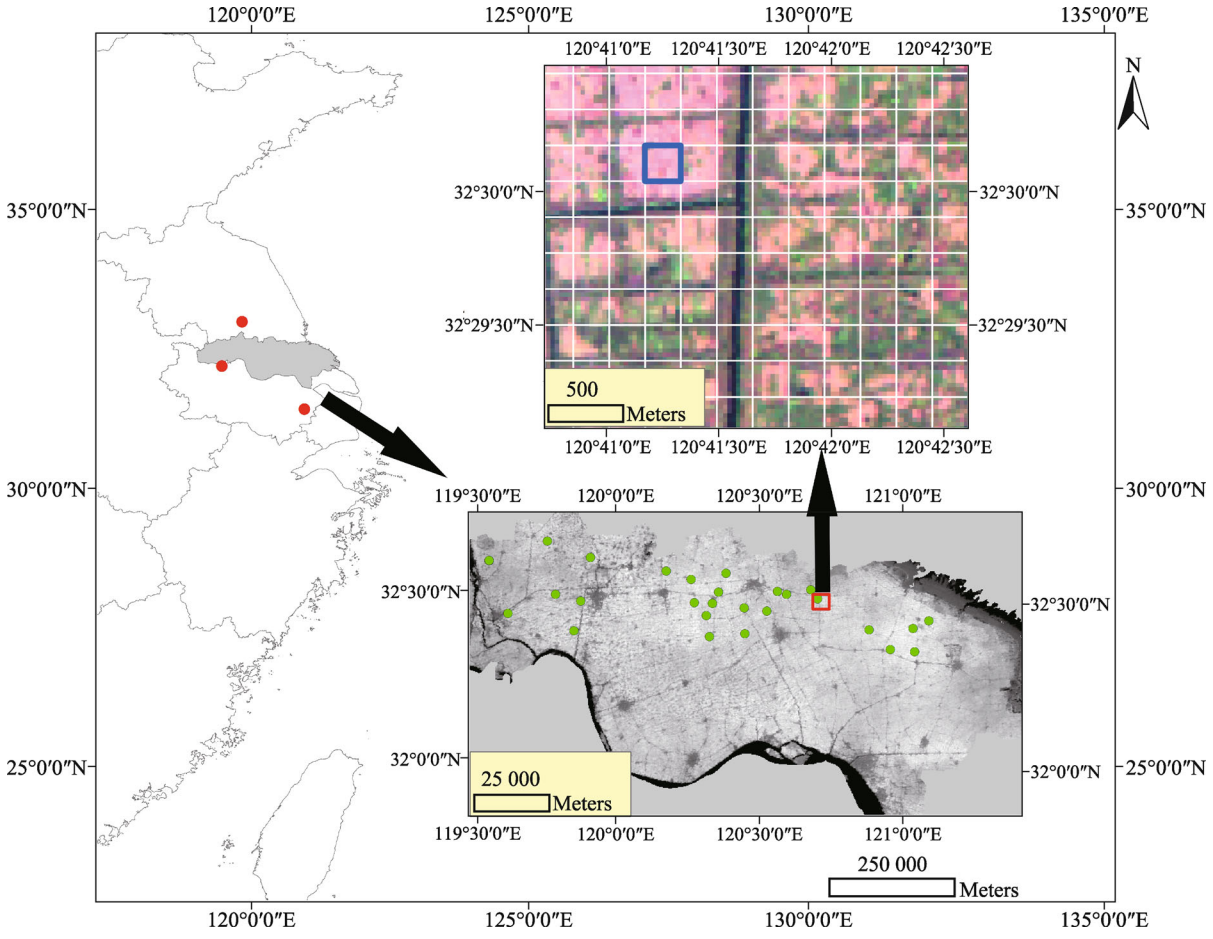

Fig. 1 Study area. The red points represent ground observation stations. The green points represent pure rice pixels. White transparent grids in the colored frame denote the MODIS pixels. The blue grid denotes one of the pure pixels. The colored background is TM data obtained on October 17 with R, G, B channels corresponding to band 5, 4, 3. A total of 28 pure MODIS pixels of bare cropland (rice-covered area) were selected for analysis.

3 Data collection and preprocessing

The 8-day NDVI images with 250-m resolution were generated from MOD09Q1 surface reflectance. Pure rice pixels of MODIS were selected by interpreting harvested paddy fields from the TM image. Frequency-based decomposition was implemented to intra-annual NDVI time series of these pixels.

3.1 Time series NDVI image

We obtained 8-Day MOD09Q1 Surface Reflectance with 250-m spatial resolution (Justice et al., 2002) for the years from 2003–2005 through the online data pool at the NASA Land Processes Distributed Active Archive Center (LPDAAC). MOD09Q1 provides Bands 1 (red) and 2 (near-infrared) at 250-m resolution in an 8-day gridded level-3 product in the Sinusoidal projection. The MODIS team has conducted radiometric correction, and the geometric error is approximately 50 m at nadir (Wolfe et al., 2002). NDVI was calculated using the red and near-infrared bands. MOD09Q1 pixels contain the best observation during an 8-day period. It was chosen based on high observation coverage, low view angle, reduced clouds or cloud shadow, and aerosol loading. Quality assessment (QA) data may help to remove those cloud-contaminated pixels. However, due to processing errors of LPDAAC, the QA for MOD09Q1 in the study area is unavailable. Thus, it is a great challenge to retrieve the crop phenology curves without QA flags, and this may help to test the robustness of the frequency-based methods in phenology estimation.

3.2 Ground observation data

We used rice phenology dates of the year 2003–2005 observed from three agriculture-meteorology stations (Fig. 1) as the reference data for assessing different methods. As the number of ground observations is small, the observations cannot represent the spatiotemporal

variations of rice phenology for selected pixels very well. Thus, we use the average planting date and harvesting date of the three observations for the years 2003−2005 as the ground truth, allowing a variation of ± 20 days. The data still has high reliability for reference of rice phenology dynamics due to small latitudinal span among the 3 stations.

3.3 Selecting pure pixels in rice-covered region

Rice planting and harvesting are the two main phenology events all through its growing season. The average planting date for the year 2003−2005 is June 17th, and the average harvesting date is October 16th. A scene of TM image taken on October 17th, 2005 (119/38) was adopted for the selection of pure MODIS pixels. The rice harvesting date was on October 16, on an average, and thus most rice-planting areas become bare cropland from that day onwards. Vectorized grids (the white grids in Fig. 1) corresponding to MODIS pixels were overlayed with the TM image to select the pure rice-covered pixels. We select the pure MODIS pixels based on visual interpretation. We first identified the bare farmlands from the TM image within each MODIS pixel, then pixel purity of MODIS was calculated. A total of 28 pixels containing more than 90% of harvested croplands were selected, and NDVI time series of these pixels were extracted and analyzed.

4 Frequency-based methods

4.1 Discrete Fourier transformation

DFT was performed to decompose the original NDVI time series data into different frequencies. New NDVI time series were reconstructed with a few frequencies. The DFT, $X(k)$, of an N-element time series $x(n)$, was defined as:

$$X(k) = \sum_{n=0}^{N-1} x(n) \mathrm{e}^{-j\frac{2\pi}{N}nk} \quad k = 0,1,2,...,N-1. \tag{1}$$

The inverse DFT was:

$$x(n) = \frac{1}{N} \sum_{k=0}^{N-1} X(k) \mathrm{e}^{j\frac{2\pi}{N}nk} \quad n = 0,1,2,...,N-1, \tag{2}$$

where, j denotes the imaginary part. We use Eq. (1) to decompose the time series data into different Fourier frequencies, and Eq. (2) to reconstruct new time series curves.

4.2 Discrete wavelet transformation

DWT decomposes a signal into a set of basis functions at different scales. By decomposing a time series into time-frequency space, one can determine both the dominant modes of variability and how those modes vary in time (Torrence and Compo, 1998).

$$W(a,b) = \int_{-\infty}^{+\infty} \frac{1}{\sqrt{a}} \psi\left(\frac{t-b}{a}\right) f(t) \mathrm{d}t, \tag{3}$$

where a is a scaling parameter, b is a shifting parameter, and denotes a mother wavelet. To allow fast numerical implementation, a and b were often sampled at dyadic sequence. In dyadic wavelet transformation, the DWT coefficients of $f(t)$ can be obtained from Eq. (4).

$$W_{j,k} = 2^{-j/2} \int_{-\infty}^{+\infty} f(t) \overline{\psi(2^{-j}t-k)} \mathrm{d}t \quad j = 0,1,...,k \in Z. \tag{4}$$

$f(t)$ can be reconstructed from the wavelet coefficients $W_{j,k}$ by means of the inverse DWT as shown in Eq. (5) (Martínez and Gilabert, 2009).

$$f(t) = \sum_{j=-\infty}^{\infty} \sum_{k=-\infty}^{\infty} W_{j,k} 2^{-j/2} \psi(2^{-j}t-k). \tag{5}$$

To remove noises, we need to identify on which scale the coefficient can better represent the noises.

4.3 Empirical mode decomposition

For a given signal $x(t)$, EMD ends up with a representation of Eq. (6)

$$x(t) = m_K(t) + \sum_{k=1}^{K} d_k(t), \tag{6}$$

where $m_K(t)$ stands for the residual and $d_k(t)$ stands for IMFs. The algorithm of EMD can be summarized as follows:

a identify all extrema of $x(t)$.

b interpolate between minima to generate the envelope $e_{\min}(t)$; and interpolate between maxima to generate the envelope $e_{\max}(t)$.

c calculate the mean $m(t)=(e_{\min}(t)+ e_{\max}(t))/2$.

d calculate the detail $d(t)= x(t)-m(t)$.

e iterate on the residual $m(t)$.

until $m(t)$ can be considered as zero-mean according to stopping criterion (Rilling et al., 2003).

To summarize the three frequency-based methods used in this study, the original time series were decomposed based on different basis functions (Fourier functions in DFT and wavelet mother functions in DWT) and rules (intrinsic oscillation in EMD). Different frequencies (Fourier frequencies in DFT, wavelet coefficients in DWT, and IMFs in EMD) can be generated and used for signal reconstruction.

The DFT, DWT, and EMD were conducted to selected time series for the year 2003−2005. The planting date and harvesting date was estimated with spline interpolation. Finally, the estimation results were assessed with ground observations.

5 Retrieving rice phenology with frequency-domain analysis

The study flow can be shown in Fig. 2. The raw MOD09Q1 data sets were used to calculate NDVI with 8-day temporal resolution and 250-m spatial resolution. There are 46 NDVI images within one year. Sampling process was implemented with the help of TM image close to harvesting date. The big noises on the NDVI time series were linearly interpolated.

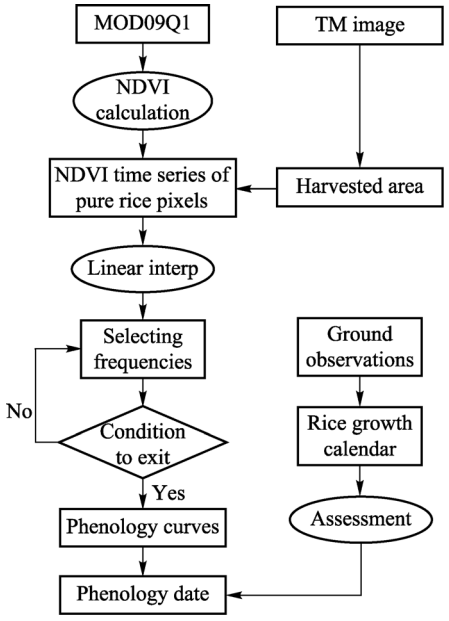

Fig. 2 Study process of rice phenology monitoring.

5.1 Linear interpolation

Clouds may cause downward fluctuations on NDVI time series. We replaced some big downward noises using linear interpolation (Fig. 3). Within rice's life cycle, it is reasonable that NDVI may change slowly. An abrupt decrease was treated as noise. We identified this noise by estimating a threshold. An earlier study (Chen et al., 2004) pointed out that most of the optimal thresholds were in the range of 0.1−0.4. If the value of a point was smaller than the values of the previous point and the next point by 0.2, the downward point was defined as an outlier. After identifying these outliers, linear interpolation was conducted to replace these noises.

5.2 Implementing frequency-based analysis

After linear interpolation, there was still some noise on the curve (Fig. 3). The estimation of special points, e.g., inflection points, requires the phenology curve to be smoother. Thus, further reconstruction of the phenology

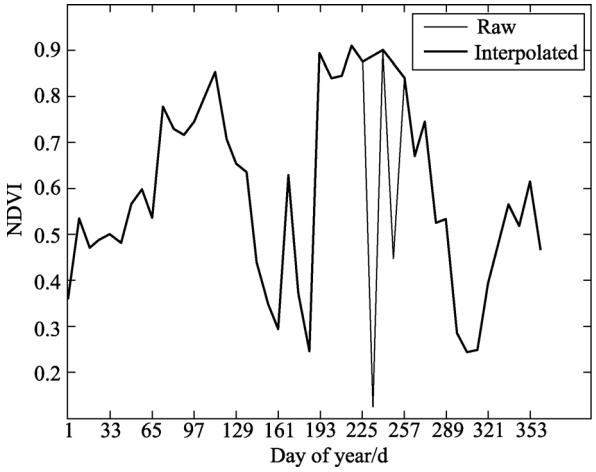

Fig. 3 Comparison of data before and after linear interpolation.

curve is required. DFT, DWT, and EMD were performed with interpolated data to generate noise-free crop phenology curves. For these frequency-based filters, we set the conditions to exit the loop for DFT, DWT, and EMD. To reconstruct the reasonable shapes of rice phenology curves, the following rules were set. These rules can be treated as the exit conditions for loops of different methods.

① The minimum NDVI value (rice planting day) between two cropping cycles should be within 17−23 points;

② There is only one peak value for the rice phenology curve and the peak should have an index within 26−32.

③ The difference between the maximum value and the minimum value for rice phenology should be larger than 0.15.

In DFT, the phenology curve was reconstructed using an inverse Fourier transformation with different Fourier frequencies. Owing to the double-cropping mode in the study area, there were two growth cycles within a year. NDVI time series were decomposed into different frequencies. Usually, the first frequency mainly captures the information of the single-cropping mode, and the second frequency the double-cropping mode. As the frequency increases, it can depict more detailed vegetation phenology information, but at the same time, it may introduce more noise. In this study, the loop starts from frequency = 1 and increases by one step until the reconstructed curve meets the exit conditions. The upper limit of frequency is 5, which means the loop will exit when frequency equals 5 if the curve still does not meet the exit conditions.

In DWT, the phenology curve was reconstructed with approximate coefficients of different scales. Most of the noise was included in "detail coefficient" with high frequencies (Fig. 5). One of the most important parts of wavelet analysis is the determination of mother function.

Crop phenology curves were reconstructed with mother wavelet "coiflet" of order 4 proposed by Sakamoto et al. (2005). In DWT, the larger the scale that is considered, the smoother the curve that can be generated. In this study, the loop starts from scale = 5 and increases by one step until the reconstructed curve meets the exit conditions. If the curve does not meet the exit conditions, the lower limit of the scale to exit the loop is scale = 1.

In EMD, the phenology curve was reconstructed with the sum of IMFs and the residual. Time series of different samples may be decomposed into 3−4 IMFs. In most cases, phenology fluctuations were located on the last two IMFs (Fig. 4). The IMFs used for reconstruction contained two growth cycles in the double-cropping area. EMD was implemented in MATLAB R2013a with the algorithm introduced by (Rilling et al., 2003). Similar to DWT and DFT, we set a loop to select the IMF in order to reconstruct ideal phenology curves. In this study, the loop starts from the last IMF and decreases by one step until the reconstructed curve meets the exit conditions. The lower limit to exit the loop is IMF = 1.

5.3 Estimating phenological stages

The phenology dates extracted from crop phenology curves are shown in Fig. 6. In previous studies, the minimal point (the first derivative equals 0 and changes from negative to positive at this point) was considered as the planting date. The inflection point where the second derivative equals 0 and changes from positive to negative was considered as the harvesting date (Sakamoto et al., 2005).

6 Results and discussion

The frequency-based methods can decompose crop NDVI time series into different frequencies. The three curves generated from EMD, DFT, and DWT represent basic trends of intra-annual vegetation cycles under the double-cropping mode (Fig. 7). The variations in estimated planting date (day of minimum value) retrieved from three methods are larger than harvesting date, as can be seen in the results reported in Table 2.

6.1 Valid estimation from different methods

There may be some spatiotemporal variations in planting and harvesting dates due to agricultural management and climatic variability. In accordance with local cultivation systems, the expected spatiotemporal variation of rice planting and harvesting days is within ±20 days. Thus, an accurate estimation should correspond to the planting date within 148−188 days centered on the average planting day of ground observations, and the inflection point corresponding to the harvesting date should fall within 270−310 days centered on the average harvesting day of ground observations. We use the percentage of effective estimations (the number of effective estimations divided by the number of all the estimations in 2003−2005) to assess the validity of different methods.

As Table 1 shows, DFT yields the best estimate of planting date (96% accuracy) but the worst estimate of harvesting date (51%). DWT can obtain the best estimate of harvesting date (89%) but worst estimate of planting date (80%). Compared with DWT and DFT, EMD can

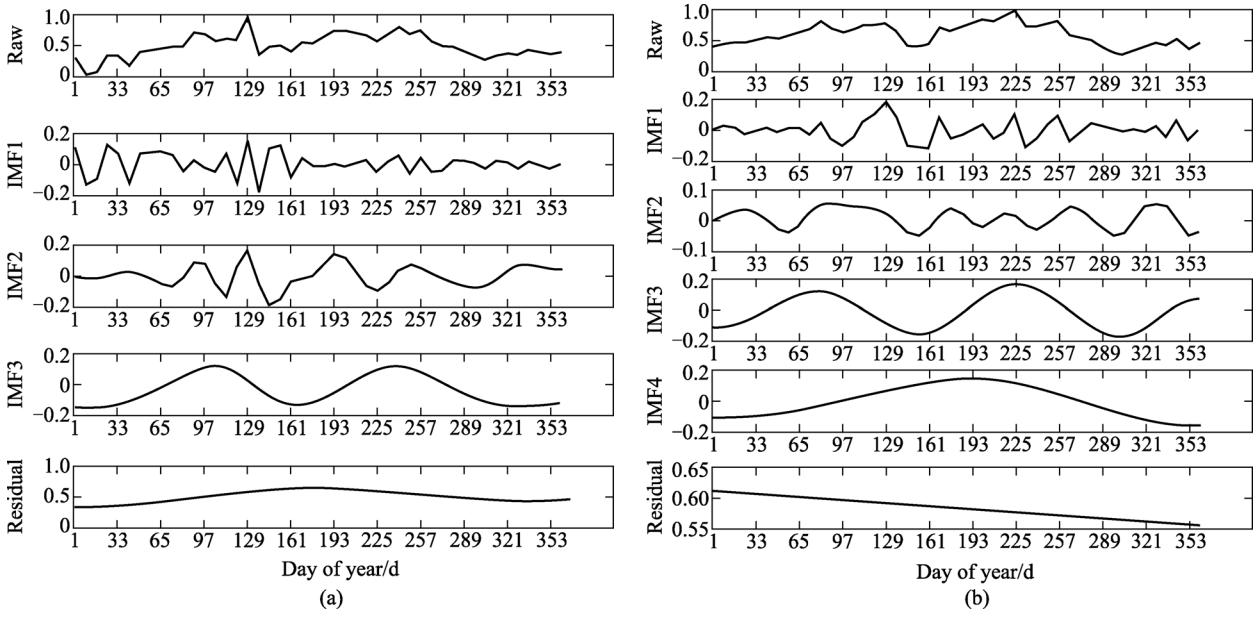

Fig. 4 EMD decomposition of NDVI time series. Noise is mainly distributed on IMF1 and IMF2. Time series were decomposed into (a) 3 IMFs and (b) 4 IMFs. Crop phenology information mainly locates on IMF3.

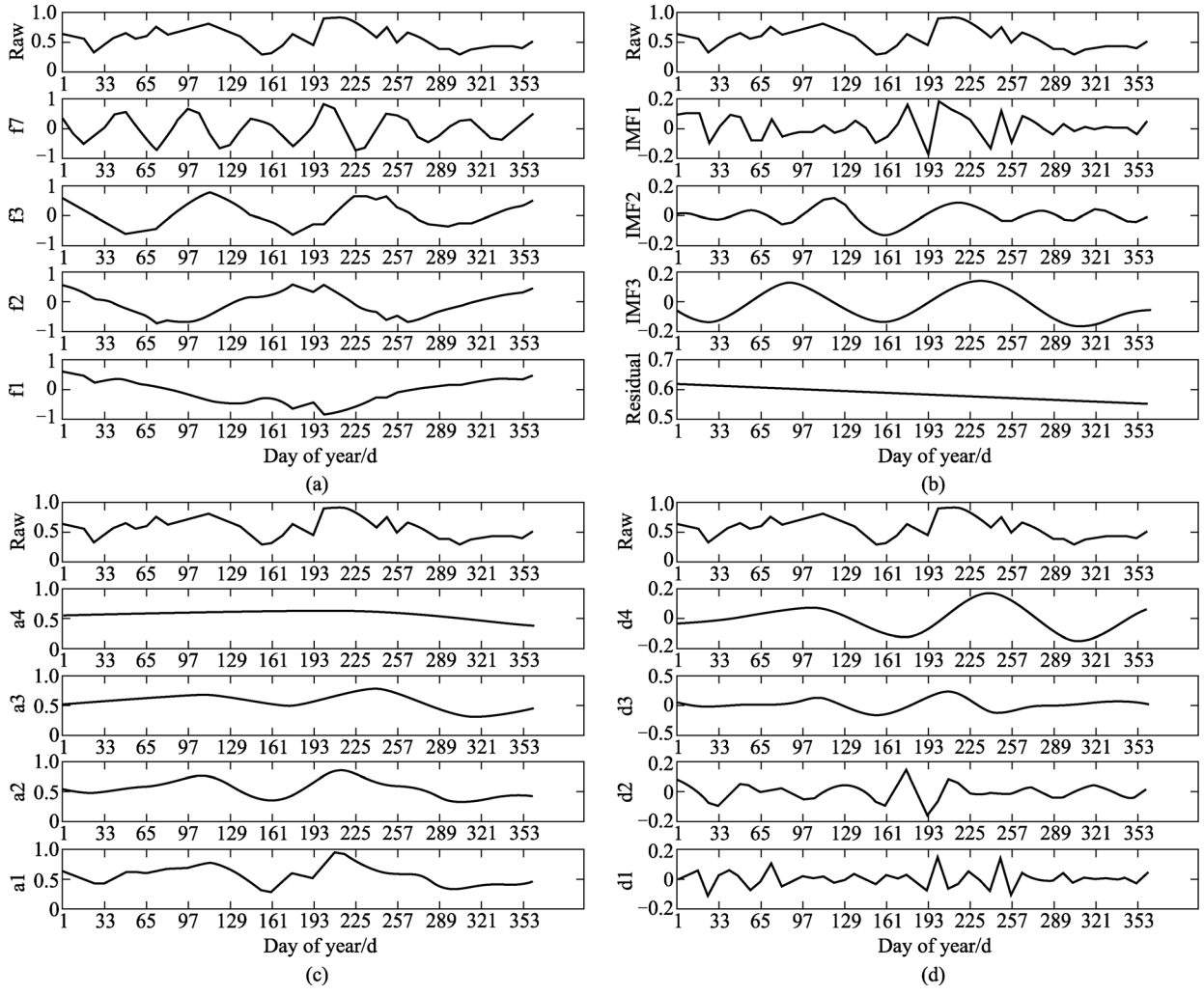

Fig. 5 Decomposition of time series data with different methods. (a) The real parts of different frequencies (f1, f2, f3, f7) from DFT, (b) three IMFs (IMF1−IMF3) from EMD, (c) the approximate coefficient of four scales (a1−a4) from DWT, and (d) the detail coefficient of four scales (d1−d4) from DWT.

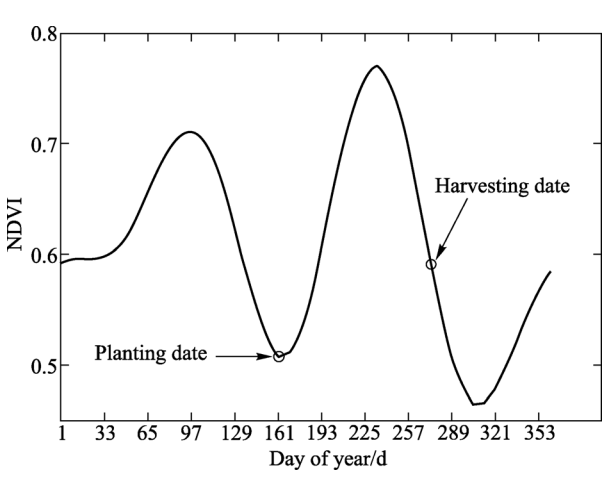

Fig. 6 Points on crop phenology curve indicating different growth stages. The phenology curve was drawn with DFT.

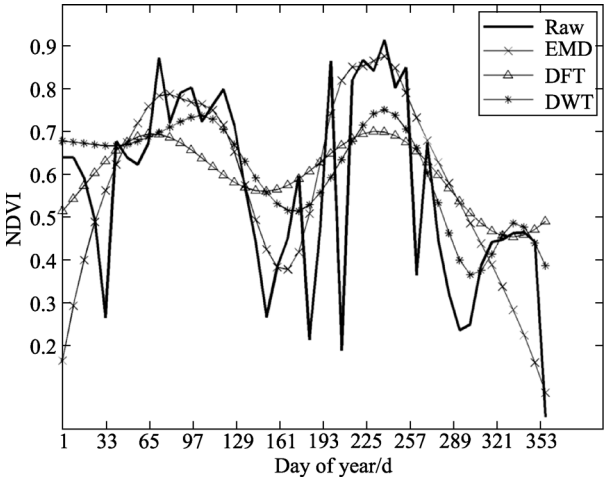

Fig. 7 Rice phenology curves reconstructed from different methods.

Table 1 The effective points retrieved from EMD, DFT, and DWT. The estimations from the year 2003–2005 were considered

Methods	Planting date		Harvesting date		Average	
	Valid points	Percentage	Valid points	Percentage	Valid points	Percentage
EMD	75	89%	60	71%	68	80%
DFT	81	96%	43	51%	62	74%
DWT	67	80%	75	89%	71	85%
Average	75	88%	60	70%	68	79%

Table 2 Standard deviation of estimations from different methods. The calculation was conducted with effective points from different methods

Methods	Year	Planting/days	Average/days	Harvesting/days	Average/days
EMD	2003	10.1	8.3	7.7	6.7
	2004	5.9		6.6	
	2005	8.9		5.7	
DFT	2003	6.4	5.7	1.7	6.7
	2004	4.3		8.0	
	2005	6.3		10.4	
DWT	2003	11.9	10.7	3.9	5.0
	2004	11.6		3.0	
	2005	8.7		8.0	
Average/days		8.2		6.1	

retrieve a medium proportion of effective estimates for planting date and harvesting date. Overall, DWT can yield the best estimates (85%) while DFT can get the worst estimates (74%) for both planting and harvesting date. Planting date (88%) is easier to estimate than harvesting date (70%). This may be due to the ease of finding the minimal point compared to an inflection point on the smoothed curve (Fig. 6). Not every smoothed curve can accurately depict the inflection point. For example, the EMD curve in Fig. 7 is not smooth enough to have an inflection point. Huang et al. (1998) shows the superiority of EMD over DWT in decomposing non-linear and non-stationary time series, while our study does not prove the superiority of EMD over DWT. This may be related to the fact that NDVI time series of rice phenology is a linear time series whose localized features can be better captured by DWT.

6.2 Variations of estimation from different methods

As Table 2 shows, DWT's estimated planting date had the largest variation (10.7 days) while the estimated harvesting date had the smallest variation (5.0 days). DFT in contrast estimated the planting date with the smallest variation (5.7 days). The STD of harvesting date (6.1 days) is less than that of planting date (8.2 days). This may be explained by the following reasons. In the selected double-cropping area, the rice planting date retrieved from phenology curves may be influenced by the former cropping curves. The former crop type may be either wheat or rapeseed. The minimum points between the double-cropping may be also influenced by different cropping systems.

6.3 The limitations of EMD in retrieving crop phenology

This study shows that IMFs selection is critical in reconstructing the EMD curve. The crop phenology information was mainly located on the last two IMFs. Crop phenology curves were reconstructed based on IMFs from EMD. EMD decomposed NDVI time series were based on the signal itself while DFT and DWT were subject to basis functions and parameters that may change with different conditions of vegetation growth. However, it was relatively difficult to find optimal IMFs to represent phenology curves from EMD because EMD was limited to fewer frequencies than DFT and DWT. In this study, the original time series of NDVI can only be decomposed into 3~4 IMFs, which is less than decomposed frequencies of DFT and the scales of DWT. Consequently, the selected IMF may not reflect the cropping phenology as detailed as DFT and DWT. Fig. 8 (b) shows that the crop phenology curve can be adequately reconstructed with the last IMF in (a); while Fig. 8 (d) shows that the crop phenology curve cannot be adequately reconstructed with either the last IMF or the last two IMFs. If reconstructed with the last IMF, the phenology curve cannot reflect the former cropping; if

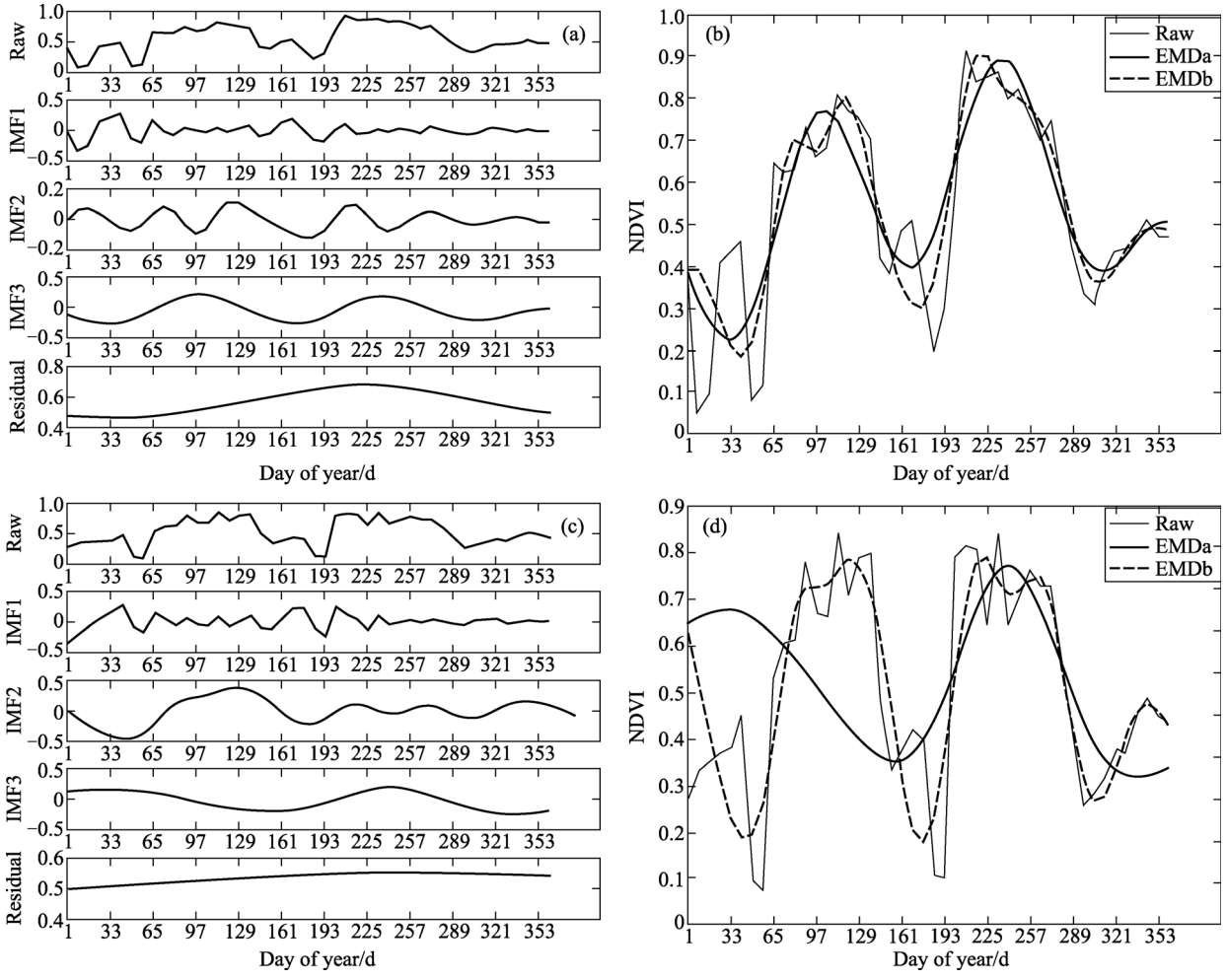

Fig. 8 Rice phenology reconstruction with different IMFs in EMD. Curves in (b) are reconstructed with IMFs in (a), and curves in (d) are reconstructed with IMFs in (c). EMDb denotes the curve reconstructed with the last two IMFs and residual; EMDa denotes the curve reconstructed with the last IMF and residual.

reconstructed with the last two IMFs, the phenology curve was not smooth enough.

6.4 Uncertainties, errors, and accuracies of estimation

The outlier estimates from different methods may be due to two reasons. 1) The limiting factors of crop growth under the double-cropping mode were more complicated than in single-cropping mode. Therefore, there were some variations of phenology that may not be reflected by the retrieved curves. 2) The parcelization of rice croplands in China may cause local variations in cultivating systems due to diverse management by different owners. Even though more than 90% of selected MODIS pixels were covered by paddy fields, there may be human-induced cultivation differences. For example, different rice species and irrigation management within a single MODIS pixel may cause spatial heterogeneity. The reconstructed phenology curve may not reflect those differences. We recommend trying multi-methods in monitoring crop phenology with remote sensing data in double-cropping areas in China to enhance the understanding of uncertainties.

The estimation results were affected by MODIS data themselves. The sampling time interval for the MOD09Q1 product from a constrained view angle-maximum value composite (CV-MVC) method was 8 days, and we used the center day to interpolate the phenology date. This may potentially contain some uncertainties. In addition, due to the complexity of the croplands in the study area, it is very difficult to select pure rice pixels. We can only select a very limited number of pure rice pixels (28 in each year).

The accuracy assessment may not be well representative of the cross-site variations of selected pixels due to the small number of ground observations (Fig. 1). However, the ground observations are still reliable as the reference

data in view of the small latitudinal span of the study area (less than 2°). Even though regional variations in cropping and diverse growth conditions may cause uncertainties in accuracy assessment, the presentation of different methodological schemes in rice phenology retrieval within the frequency domain of NDVI time series may facilitate agronomists' and engineers' future crop phenology monitoring in double-cropping regions in China.

7 Conclusions

In this paper, we examined the accuracy of DFT, DWT, and EMD in retrieving rice phenology in double-cropping in Jiangsu Province, China. MODIS 8-day NDVI time series were used to characterize crop phenology. This study sheds light on double-cropping phenology retrieval in the frequency domain from differing methodological perspectives. The following main conclusions can be drawn. 1) Multi-temporal MODIS NDVI data combined with frequency-based analysis can retrieve rice phenology dates with on average 79% valid estimates in cloudy and double-cropping areas of China even when lacking information on quality assessment of MOD09Q1. 2) Rice phenology in double-cropping China is mainly located on the last 2 IMFs of EMD and the first 2–3 frequencies of DFT and DWT. For more accurate rice phenology retrieval, these frequencies from different methods should be incorporated. 3) In double-cropping China, the estimate of rice planting dates (standard deviation = 8.2 days) has larger variations than that of rice harvesting dates (standard deviation = 6.1 days), while rice planting dates can be more accurately estimated (88%) than harvesting dates (70%). The overall sorting result for accuracy of the different methods is DWT (85%) > EMD (80%) > DFT (74%) in the study area. 4) Further research is needed, including studying the feasibility of frequency-based methods in monitoring phenology dynamics for other crop types and the effect of cropland complexity (e.g., parcelization and individual agriculture management) on phenology estimation from remotely sensed data.

Acknowledgements This study was funded by the National Basic Research Program of China (No. 2015CB954103), National Sci-Tech Support Plan (2012BAD20B0103). The authors are grateful to China Meteorological Agency, USGS and NASA for contributions to data collection. Thank Prof. Jingfeng Huang in Zhejiang University for his comments in the publication process.

References

Andres L, Salas W, Skole D (1994). Fourier analysis of multi-temporal AVHRR data applied to a land cover classification. Int J Remote Sens, 15(5): 1115–1121

Carrao H, Gonalves P, Caetano M (2010). A nonlinear harmonic model for fitting satellite image time series: analysis and prediction of land cover dynamics. IEEE Trans Geosci Rem Sens, 48(4): 1919–1930

Chan K K Y, Xu B (2013). Perspective on remote sensing change detection of Poyang Lake wetland. Ann GIS, 19(4): 231–243

Chen C F, Chen C R, Son N T (2012). Investigating rice cropping practices and growing areas from MODIS data using empirical mode decomposition and support vector machines. GIsci Remote Sens, 49 (1): 117–138

Chen C, Son N, Chang L, Chen C (2011). Classification of rice cropping systems by empirical mode decomposition and linear mixture model for time-series MODIS 250 m NDVI data in the Mekong Delta, Vietnam. Int J Remote Sens, 32(18): 5115–5134

Chen J, Jonsson P, Tamura M, Gu Z, Matsushita B, Eklundh L (2004). A simple method for reconstructing a high-quality NDVI time-series data set based on the Savitzky-Golay filter. Remote Sens Environ, 91 (3−4): 332–344

Cleland E, Chuine I, Menzel A, Mooney H, Schwartz M (2007). Shifting plant phenology in response to global change. Trends in Ecology and Evolution, 22(7): 357–365

Coughlin K, Tung K (2004). 11-year solar cycle in the stratosphere extracted by the empirical mode decomposition method. Adv Space Res, 34(2): 323–329

Delbart N, Le Toan T, Kergoat L, Fedotova V (2006). Remote sensing of spring phenology in boreal regions: a free of snow-effect method using NOAA-AVHRR and SPOT-VGT data (1982−2004). Remote Sens Environ, 101(1): 52–62

Genovese G, Vignolles C, Nègre T, Passera G (2001). A methodology for a combined use of normalised difference vegetation index and CORINE land cover data for crop yield monitoring and forecasting. A case study on Spain. Agronomie, 21(1): 91–111

Huang N E, Shen Z, Long S R, Wu M C, Shih H H, Zheng Q, Yen N C, Tung C C, Liu H H (1998). The empirical mode decomposition and the Hilbert spectrum for nonlinear and non-stationary time series analysis. Proceedings of the Royal Society of Medicine, 454(1971): 903–995

Huang N, Shen S (2005). Hilbert-Huang Transform and Its Applications. Singapore: World Scientific Pub Co Inc.

Huete A, Didan K, Miura T, Rodriguez E P, Gao X, Ferreira L G (2002). Overview of the radiometric and biophysical performance of the MODIS vegetation indices. Remote Sens Environ, 83(1−2): 195–213

Ito E, Araki M, Tith B, Pol S, Trotter C, Kanzaki M, Ohta S (2008). Leaf-shedding phenology in lowland tropical seasonal forests of cambodia as estimated from NOAA satellite images. IEEE Trans Geosci Rem Sens, 46(10): 2867–2871

Ivanov P, Rosenblum M, Peng C, Mietus J, Havlin S, Stanley H, Goldberger A (1996). Scaling behaviour of heartbeat intervals obtained by wavelet-based time-series analysis. Nature, 383(6598): 323–327

Justice C, Townshend J, Holben B, Tucker C (1985). Analysis of the phenology of global vegetation using meteorological satellite data. Int J Remote Sens, 6(8): 1271–1318

Justice C, Townshend J, Vermote E F, Masuoka E, Wolfe R E, Saleous N, Roy D P, Morisette J T (2002). An overview of MODIS Land data processing and product status. Remote Sens Environ, 83(1−2): 3–15

Kobayashi H, Dye D (2005). Atmospheric conditions for monitoring the long-term vegetation dynamics in the Amazon using normalized difference vegetation index. Remote Sens Environ, 97(4): 519–525

Lobell D B, Burke M B, Tebaldi C, Mastrandrea M D, Falcon W P, Naylor R L (2008). Prioritizing climate change adaptation needs for food security in 2030. Science, 319(5863): 607–610

Lu X, Liu R, Liu J, Liang S (2007). Removal of noise by wavelet method to generate high quality temporal data of terrestrial MODIS products. Photogramm Eng Remote Sensing, 73(10): 1129–1139

Martínez B, Gilabert M A (2009). Vegetation dynamics from NDVI time series analysis using the wavelet transform. Remote Sens Environ, 113(9): 1823–1842

Mo X, Liu S, Lin Z, Xu Y, Xiang Y, McVicar T (2005). Prediction of crop yield, water consumption and water use efficiency with a SVAT-crop growth model using remotely sensed data on the North China Plain. Ecol Modell, 183(2−3): 301–322

Molla M, Rahman M, Sumi A, Banik P (2006). Empirical mode decomposition analysis of climate changes with special reference to rainfall data. Discrete Dyn Nat Soc, 2006: 1–17

Peng S, Tang Q, Zou Y (2009). Current status and challenges of rice production in China. Plant Prod Sci, 12(1): 3–8

Percival D, Walden A (2006). Wavelet Methods for Time Series Analysis.Cambridge University Press

Qian S, Chen D (1999). Joint time-frequency analysis. IEEE Signal Process Mag, 16(2): 52–67

Raddatz R, Cummine J (2003). Inter-annual variability of moisture flux from the prairie agro-ecosystem: impact of crop phenology on the seasonal pattern of tornado days. Boundary-Layer Meteorol, 106(2): 283–295

Rilling G, Flandrin P, Goncalvés P (2003). On empirical mode decomposition and its algorithms. In Proceedings of the 6th IEEE/EURASIP Workshop on Nonlinear Signal and Image Processing, Grado, Italy 2003

Sakamoto T, Van Nguyen N, Ohno H, Ishitsuka N, Yokozawa M (2006). Spatio–temporal distribution of rice phenology and cropping systems in the Mekong Delta with special reference to the seasonal water flow of the Mekong and Bassac rivers. Remote Sens Environ, 100(1): 1–16

Sakamoto T, Yokozawa M, Toritani H, Shibayama M, Ishitsuka N, Ohno H (2005). A crop phenology detection method using time-series MODIS data. Remote Sens Environ, 96(3−4): 366–374

Santoso S, Powers E J, Grady W M, Hofmann P (1996). Power quality assessment via wavelet transform analysis. IEEE Trans Power Deliv, 11(2): 924–930

Schmidhuber J, Tubiello F N (2007). Global food security under climate change. Proc Natl Acad Sci USA, 104(50): 19703–19708

Shen J, Liu J, Lin X, Zhao R, Xu S (2011). Cropland extraction from very high spatial resolution satellite imagery by object-based classification using improved mean shift and one-class support vector machines. Sens Lett, 9(3): 997–1005

Slayback D, Pinzon J, Los S, Tucker C (2003). Northern hemisphere photosynthetic trends 1982−99. Glob Change Biol, 9(1): 1–15

Tan G, Shibasaki R (2003). Global estimation of crop productivity and the impacts of global warming by GIS and EPIC integration. Ecol Modell, 168(3): 357–370

Tao F, Yokozawa M, Xu Y, Hayashi Y, Zhang Z (2006). Climate changes and trends in phenology and yields of field crops in China, 1981–2000. Agric Meteorol, 138(1−4): 82–92

Torrence C, Compo G (1998). A practical guide to wavelet analysis. Bull Am Math Soc, 79(1): 61–78

Vasudevan K, Cook F (2000). Empirical mode skeletonization of deep crustal seismic data: theory and applications. J Geophys Res, D, Atmospheres, 105(B4): 7845–7856

Wang H S, Chen J S, Wu Z F, Lin H (2012a). Rice heading date retrieval based on multi-temporal MODIS data and polynomial fitting. Int J Remote Sens, 33(6): 1905–1916

Wang H S, Lin H, Chen J S, Chen F L (2012b). Study on the relationship between sub-pixel percentage cover and multi-temporal NDVI. Int J Remote Sens, 33(17): 5615–5628

Wang H S, Lin H, Liu D S (2014). Remotely sensed drought index and its responses to meteorological drought in Southwest China. Remote Sens Lett, 5(5): 413–422

Wang H S, Rogers J C, Munroe D K (2015). Commonly used drought indices as indicators of soil moisture in China. J Hydrometeorol, 16 (3): 1397–1408

Wolfe R E, Nishihama M, Fleig A J, Kuyper J A, Roy D P, Storey J C, Patt F S (2002). Achieving sub-pixel geolocation accuracy in support of MODIS land science. Remote Sens Environ, 83(1−2): 31–49

Xiao X M, Boles S, Liu J Y, Zhuang D F, Frolking S, Li C S, Salas W, Moore B III (2005). Mapping paddy rice agriculture in southern China using multi-temporal MODIS images. Remote Sens Environ, 95(4): 480–492

You X, Meng J, Zhang M, Dong T (2013). Remote sensing based detection of crop phenology for agricultural zones in China using a new threshold method. Remote Sens, 5(7): 3190–3211